UNIVERSITÉ LAVAL

System Level Design of a Full-Duplex Wireless Transceiver for Brain-Machine Interfaces

Hadi Bahrami, S. Abdollah Mirbozorgi, An T. Nguyen, Benoit Gosselin, and Leslie A. Rusch

IEEE Transactions on Microwave Theory and Techniques, (Volume: 64, Issue: 10, Oct. 2016)

Doi: 10.1109/TMTT.2016.2600301

https://ieeexplore.ieee.org/abstract/document/7560668/

System Level Design of a Full-Duplex Wireless Transceiver for Brain-Machine Interfaces

H. Bahrami, *Student Member, IEEE,* S.A. Mirbozorgi, *Student Member, IEEE*, T. A. Nguyen, B. Gosselin, *Member, IEEE,* and Leslie A. Rusch, *Fellow, IEEE*

***Abstract*— We propose a new wireless communication architecture for implanted systems that simultaneously stimulate neurons and record neural responses. This architecture can support large numbers of electrodes (>500), providing 100 Mb/s for the downlink of stimulation signals, and Gb/s for the uplink neural recordings. We propose a full-duplex transceiver architecture that shares one antenna for both ultra-wideband (UWB) and the 2.45 GHz ISM band. A new pulse shaper is used for the Gb/s uplink to simplify transceiver design, while supporting several modulation formats with high data rates. To validate our system level design for brain-machine interfaces (BMI), we present an ex-vivo experimental demonstration of the architecture. While the system design is for an integrated solution, the proof-of-concept demonstration uses discrete components. Good bit error rate performance over a biological channel at 0.5, 1, and 2 Gbps data rates for uplink telemetry (UWB) and 100 Mb/s for downlink telemetry (2.45 GHz band) are achieved.**

***Index Terms*—Neural recording and stimulating, Full-Duplex, Downlink, Uplink, Ultra-wideband (UWB), ISM, Brain machine interface.**

I. Introduction

IMPLANTABLE wireless transceivers are an essential part of implanted neural recording systems used for treatment and for research on neurological impairments [1-8]. Simultaneous neural stimulating and recording systems in large scale require many electrodes interfaced, perhaps permanently, to the central and peripheral nervous systems. In neural recording and stimulating applications, increasing the number of electrodes enhances understanding of the targeted part of the brain [9].

Wireless implantable devices can be powered by two different methodologies: 1) with an un-chargeable battery or energy harvester, or 2) wirelessly from external sources by an antenna or an inductive coil [10-15]. Since we target permanent implants for a high number of electrodes, we do not consider the first option. The second option can be divided into partially passive and fully passive subgroups. The high bit rates we target preclude the use of fully passive methods: where neuropotentials modulate an externally generated carrier and the modulated carrier is backscattered to an external receiver. While the fully passive circuits can reduce risks related to power dissipation in implants (they dissipate little of the induced power), analog modulation is incompatible with large-scale neural recording systems.

We therefore focus on passive powering which is suitable for permanent implants and can provide enough (milliwatts) power for an implanted device. In wireless BMI transceivers with the passive power systems, conventionally three separate links have been employed: one power inductive link and two separate communications subsystems (uplink and downlink), as shown in Fig.1-a [8, 16, 17].

Inductive data links are utilized when the required data rate is low, on the order of a few Mb/s [16-17]. At low frequencies, unlicensed bandwidth is limited, pushing high speed links to higher RF frequencies. To achieve a higher data rate for the uplink in a neural recording system, an ultra-wideband RF link was utilized instead of an inductive approach; the inductive approach was kept for the downlink [7-8]. As the number of electrodes increases, the downlink needs wider bandwidth (and hence a higher RF frequency) to be able to support 100 Mb/s data rates. Recently, we proposed 2.45 GHz industrial, scientific and medical (ISM) band as a downlink [18]. We will show in this paper that the 2.45 GHz downlink receiver can be operated in full duplex with a high data rate ultra-wideband band (UWB) uplink transmitter.

The most important features for the implanted circuit are small size and very low power consumption [1-7]. To achieve these goals we modify the traditional use of separate uplink and downlink subsystems, and propose a full-duplex data transceiver, with one dual band RF bidirectional data link. We avoid a power-hungry circulator by considering a diplexer. The diplexer is not the conventional type using band pass filtering, but a stripped down version that capitalizes on pulse shaping of the transmitted signal to take advantage of the low noise amplifier (LNA) filtering feature at the implanted downlink receiver. We shape the transmitted pulse to put most energy between 3.1-7 GHz. This also allows for good isolation from the 2.45 GHz, achieving low crosstalk between uplink and downlink. Because the transmitted pulse in an implant-to-air channel faces high insertion loss at 7-10.6 GHz [19, 20], shaping the pulse between 3.1-7 GHz and focusing energy in this subband actually enhances the uplink power efficiency compared to covering the entire UWB band. Our approach yields much simpler hardware than traditional full-duplex methods (using a circulator or conventional diplexer): fewer components, leading to greater power efficiency and smaller size - important properties for biomedical applications.

The final enabling element for our architecture is an antenna

This work was supported in part by the Natural Sciences and Engineering Research Council of Canada, by the hSITE Strategic Network and by the Microsystems Strategic Alliance of Québec. The authors are with the ECE Department, Université Laval, Québec, QC G1V 0A6, Canada (phone: +1 (418) 656-2131; fax: +1 (418) 656-3159; email: hadi.bahrami-abarghouei.1@ulaval.ca).

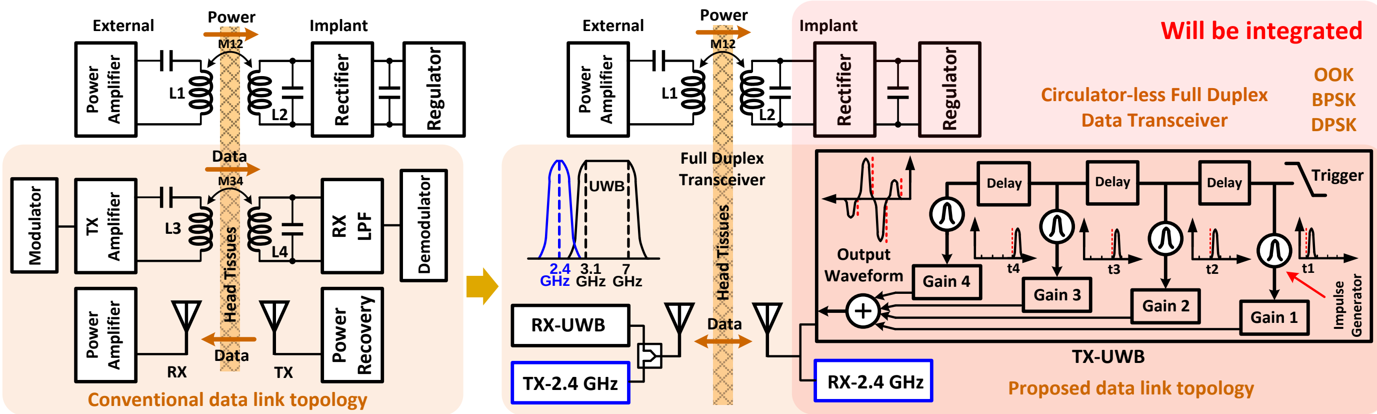

(a) (b)

Fig. 1. Brain-machine interface solutions: (a) conventional architecture with separate uplink transmitter and downlink receivers for), and (b) the proposed full-duplex, dual-band transceiver.

which covers both frequency bands with small size and good performance in a channel composed of biological materials. We developed and fabricated antennas, one implantable and one external, designed specifically for transcranial channels, which were presented in [19]. The antennas for this work were designed for dual bands, supporting both uplink and downlink.

We investigate achievable data rates of the proposed wireless links via ex vivo experiments with discrete components and biological tissues as the transmission media. We examine data rates of 0.5, 1 and 2 Gbps for the uplink. For the downlink (stimulation signals) we consider only on-off keying (OOK) at 100 Mb/s. We confirm that acceptable bit error rates (BER) can be achieved at these rates. These results greatly outstrip previous data rates for biological channels, such as 80 Mb/s for wireless implant-to-air data communications for gastro applications [21]. In that work, a multiband orthogonal frequency division modulation (MB-OFDM) was used, which consumes more power than impulse-radio UWB.

In summary our contributions are: 1) proposing a new full-duplex data transceiver architecture (for simultaneous neural recording and stimulation) with one antenna and without using a conventional diplexer or circulator, and 2) for the first time demonstrating nearly simultaneous high-speed transmissions in both 2.45 GHz-ISM and UWB bands.

In section II, we present an overview of the proposed system. In section III we describe the experimental implementation of the proposed architecture with discrete components, including an ex vivo emulation of the biological channel. Section IV presents several options for signal modulation. In section V we present BER performance. In section VI we motivate integration of the proposed architecture. Finally, conclusions are drawn in section VII.

II. System Architecture

As shown in Fig. 1-a, to date two separate communications subsystems are used for uplink and downlink data transmission. We propose a full-duplex data transceiver architecture which consists of one dual band RF bidirectional subsystem. This architecture requires fewer components (thus minimizing size and power consumption) by exploiting a small set of efficient and integrable components: a single antenna, an LNA that doubles as a bandpass filter, and a pulse shaper formed from delay elements and amplifiers. In this section we motivate the selection of this set of components, and contrast them with other solutions available in the literature. In section III we present an experimental proof-of-concept demonstration for this architecture (destined for integration) using discrete components.

Fig. 1-b shows a block diagram of the proposed transceiver supporting a bidirectional, high-data rate link through the head for neural stimulation and recording. The integrated solution will include a UWB pulse shaping transmitter and a 2.45 GHz receiver with an LNA with limited passband. The design of the external system, not considered here, is less demanding than the implantable system; it need not be biocompatible, and size and power consumption requirements are greatly relaxed. Compared to prior solutions, our architecture eliminates one antenna and an inductive link.

A. *Simplified Diplexer*

To replace two separate data links by one bidirectional data link, the transceiver must operate in full-duplex architecture (stimulation and simultaneous recording). Typically circulators or diplexers are used to implement a full-duplex transceiver (FDT) [22-27]. As a passive circulator uses ferrite materials, to have a CMOS compatible solution for integration an active circulator would be required [22-24]. Active circulators attenuate the signal at least 3 dB, increase size and power consumption, and decrease the signal-to-noise ratio of the receiver. Another solution might be implementing a conventional diplexer (two sharp band-pass filters) to separate the frequency bands [25-27]. The narrow band frequency band must be close to the UWB band for coverage by a single antenna (TX and RX). Implementing filters to operate in these two bands in CMOS technology would require significant space and add loss to transmitted and received signals.

To avoid the two sharp band-pass filters in a conventional diplexer, we propose a simplified diplexer where two separate frequency bands are supported by exploiting pulse shaping elsewhere in the transceiver. We propose one dual band transceiver to replace separate 1) 2.45 GHz-ISM band down link, and 2) UWB uplink. The UWB band (uplink) and 2.45 GHz-ISM band (downlink) were chosen for the communications bands because 1) the two frequency bands are close enough to be covered by a single antenna, and 2) they are readily available unlicensed bands per Federal Communications Commission (FCC) regulations. We show in the inset in Fig. 1-b the spectra of a UWB and a 2.45 GHz-ISM signal.

We propose implementing a FDT by 1) shaping the UWB pulse and 2) exploiting the LNA 2.45 GHz passband. The UWB pulse (see next section) is sculpted to have a spectrum beginning at 3.1 GHz. This signal is routed to the implanted antenna. This signal therefore also propagates to the 2.45 GHz receiver. Within that receiver is a low noise amplifier (LNA) designed to operate at 2.45 GHz for reception of uplink signals. The LNA has a limited passband, rejecting any UWB signal components (high impedance in UWB). Also, when the 2.45 GHz modulated signal is received by the implanted antenna, the signal is facing with high impedance output of UWB transmitter and it is routed to the 2.45 GHz LNA. By this architecture, we can have two separated bands with a good isolation between them. The FDT thus avoids use of a circulator or traditional (separate band pass filters) diplexer.

B. UWB Pulse Shaping

UWB impulse radio (UWB-IR) transmits information through short nanoseconds baseband pulses without employing a carrier, leading to advantages such as low complexity, and low power consumption [28, 29]. To generate a UWB pulse, a number of methods are available. The choice is affected by several factors such as power consumption, simplicity in implementation, modulation scheme achievable, bit error rate (BER), data rate and so on. Pulse filtering method because of using inductors in their implementation needs larger space than shaping the pulse [29]. Among different pulse shapes, the Gaussian pulse and its derivatives have a desirable compromise in frequency and time-bandwidth [29]. Gaussian derivatives are widely used in UWB transmitters; their center frequency is increased when taking an additional derivative and their spectrum bandwidth is optimized by tuning the pulse time duration [29].

We optimize the transmitted pulse subject to multiple constraints. The first one is efficient exploitation of the FCC mask. Second is isolating the transmitter and receiver in our full-duplex structure. The third is matching the frequency response of the biological communications channel. EM waves see more loss at higher frequencies in our channel; we should try to put more power in lower band of UWB band (3.1-7 GHz). And finally, the achieved pulse duration should be short to support high data rates (to avoid intersymbol interference). We target pulses with 500 ps duration to support data rates as high as 2 Gbps.

To shape the UWB pulse, the amplitude and the time duration of the fifth derivative of a Gaussian pulse is manipulated. The optimized pulse is generated by summing time-shifted Gaussian pulses algorithm as shown in Fig. 1b. This architecture promises a low power implementation because of its simplicity in comparing with other pulse shaping method [30-33]. To provide the systems designer maximum flexibility this architecture has the added advantage of supporting three signaling methods: on-off keying (OOK), phase-shift keying (BPSK), and differential phase-shift keying (DPSK). Four impulses are used to shape and generate the required UWB signal for transmitting logical “1” data during OOK modulation. To produce BPSK

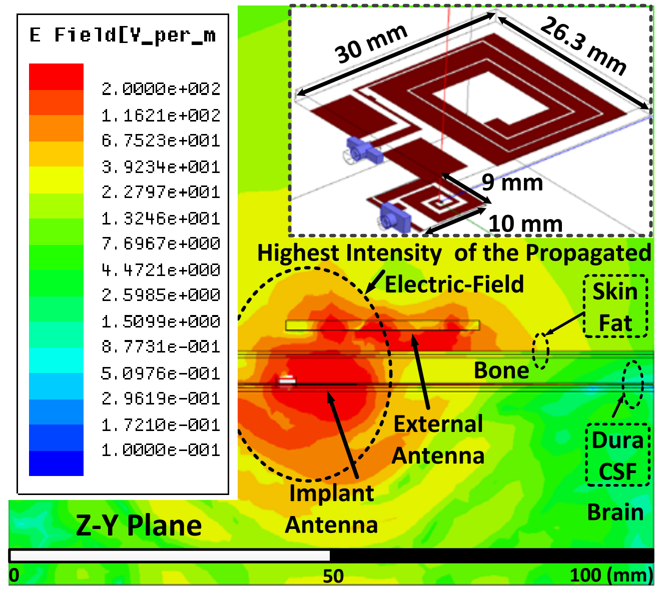

Fig. 2. Radiated E-field while implant and external antennas are communicating through biological tissues in Z-Y plane in HFSS.

and DPSK modulated signals, a similar algorithm is used, producing the same signal with a 180° phase difference when logical 0” data is transmitted.

The choice of modulation scheme depends on the required BER and data rate, power consumption and system complexity. There is a trade-off between complexity and power consumption, leading us to consider both coherent and incoherent architectures. Coherent detection requires more complex circuitry which results in higher power consumption; incoherent detection is less complex, which results in lower power consumption, but worse BER performance [34]. We consider binary phase shift keying (BPSK: coherent), differential phase shift keying (DPSK: incoherent) and on-off keying (OOK: incoherent) modulations for the uplink. DPSK has the low complexity of incoherent detection and has only a 1 dB power penalty vis-a-vis BPSK for an additive white Gaussian noise channel. A 3 dB power penalty is incurred for OOK [34].

C. Antenna Design

The final enabling element for our architecture is an antenna which covers both frequency bands with small size and good performance in biological materials. We require one implantable and one external, designed specifically for transcranial channels. We designed and fabricated spiral antennas that cover 2-11 GHz frequency band (both ISM and UWB bands) using ANSYS HFSS (a commercial finite element method solver). The fabrication and simulation results, the biological model, measurement set-up, and the material used for their fabrication are all provided in more detail in [19]. We plot in Fig. 2 the propagated electric-field between the antennas (TX and RX). The illustration shows placement of both antennas and the layers of inhomogeneous model used in ANSYS HFSS. The highest electric-field intensity is localized close to the antennas, leading to higher coupling between the antennas, and thus higher received signal-to-noise ratio (SNR). This model is used for both antenna design and for assessing transfer of heat to surrounding tissue, as explained in the next subsection.

D. *Average Specific Absorption Rate*

Average Specific Absorption Rate (ASAR) describes the electromagnetic energy that is absorbed in biological tissues and is a critical parameter for assessing the tissue-safety of implant-air wireless communications. The peak 1-g ASAR spatial distribution is simulated in HFSS for implanted antennas in 3.1-7 GHz frequency range (transmitter for uplink) and external antenna in 2.45 GHz-ISM band (transmitter for downlink). The ASAR is calculated for the implanted antenna transmitting on the UWB band, and for the external antenna transmitting on the 2.45 GHz band. The American National Standards Institute (ANSI) limitations for a maximum peak 1-g ASAR of 1.6 W/kg [35] translates into the following average radiated power: 6.4 mW (8 dBm) for the implanted antenna and 9 mW (9.5 dBm) for the external antennas. The ASAR for the external antenna is calculated assuming the antenna is placed 0.7 mm from the skin. Sending more power can dam age the biological tissues.

III. Experimental Proof-of-Concept

In the previous section we proposed an architecture that can be integrated in CMOS technology in smaller size and with lower power consumption than previously proposed systems. In this section we use test equipment and discrete components to investigate performance (achievable bit rate) of this new system level design. Our choice of discrete components emulates the integrated solutions. We test several modulation formats and measure bit error rate when propagating through animal tissue in an ex-vivo trial. To emulate the human head, the implanted and external antennas are separated by animal brain, bone, fat, and skin tissues harvested within one day of death. The ex-vivo setup which is used in this work is discussed in more detail in [19, 20].

Test equipment and discrete components for our test set-up are shown in Fig. 3-a. An arbitrary waveform generator (AWG) is programmed to generate the uplink UWB pulse, a pulse shape resembling that which would be produced by the architecture in Fig. 1. Note we use an AWG for experimental convenience, but the pulse shaper will be implemented in CMOS technology for the integrated solution [32, 33]. The UWB pulse is modulated by a pseudorandom binary sequence (PRBS) of order 15 by the arbitrary waveform generator. One million bits are transmitted using OOK, BPSK, or DPSK modulation. An attenuator is used at the transmitter for sweeping the signal-to-noise ratio (SNR) in the receiver. The attenuator is followed with a UWB band-pass filter to achieve high impedance outside its supported frequency band. The uplink signal is transmitted through the animal tissue. At the external receiver, a 3 dB power divider (22 dB isolation) is used between the two summation ports. The signal is amplified with an ultra-wideband low noise amplifier (LNA) with 27 dB flat gain and noise figure (NF) 4 dB. The uplink signal is captured by a real-time oscilloscope to be analyzed off-line in MATLAB - MathWorks.

In the downlink transmitter, the output of bit pattern generator (PRBS of order 15) running at 100 Mb/s is mixed with a 2.45 GHz tone, followed by an attenuator used for sweeping the SNR. The downlink signal is transmitted through the animal tissue. The 2.45 GHz signal received by the implanted antenna is rejected by the UWB bandpass filter before the uplink transmitter and is diverted to the implanted receiver which is 50 Ω

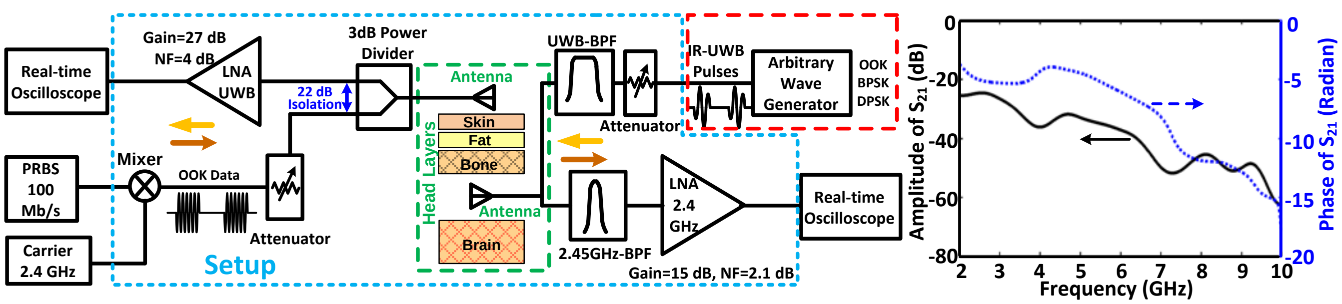

(a) (b)

Fig. 3. (a) Block digram of the system level implementation of the proposed link, and (b) the measured frequency response of the wireless channel.

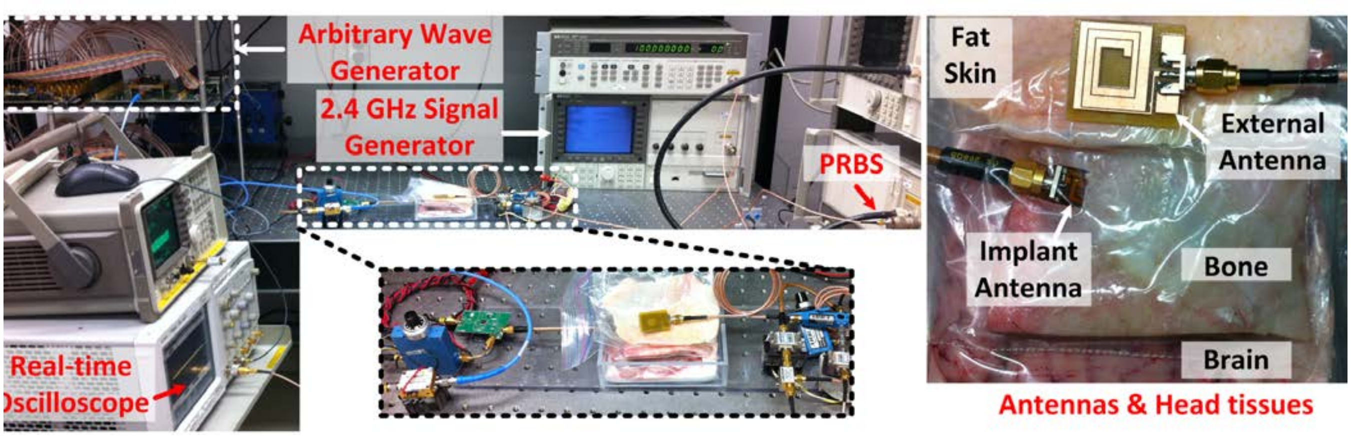

Fig. 4. Set-up for data communications.

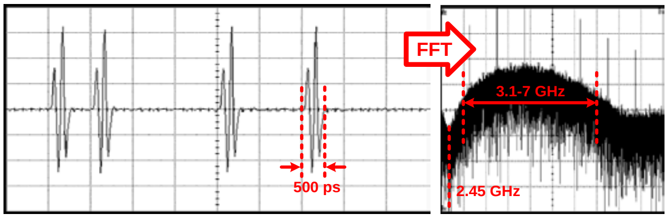

(a) (b)

Fig. 5. Measurment result: (a) OOK modulation waveform in AWG output for 500 Mb/s (b) its spectrum.

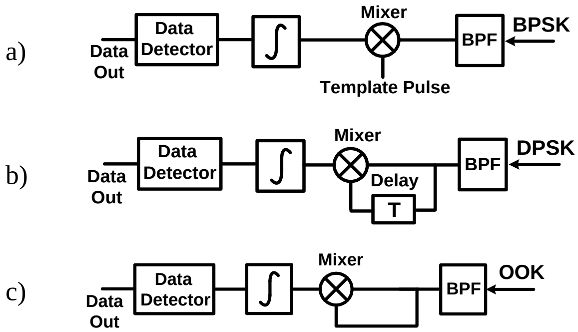

Fig. 6. Receiver blocks implemented in MATLAB (off-line processing) for (a) BPSK, (b) DPSK, and (c) OOK.

matched. A discrete band-pass filter centered at 2.45 GHz with sharp cutoff is used to emulate the passband of a LNA specially designed for this application. The LNA has NF=2.1 dB and a gain 15 dB. The amplified signal is captured by a real-time oscilloscope for processing offline in MATLAB.

We fabricated the implanted antenna on flexible PCB and the external antenna on rigid FR4 PCB [19]. 50-Ω SMA connectors connect the antennas to the other equipment, as shown in Fig. 4. To emulate the head environment, the following animal tissues are used: skin (1 mm), fat (0.5 mm), bone (6 mm), and brain (30 mm), thicknesses chosen to mimic typical human head tissues [36]. We measured and plot in Fig. 3-b the frequency response of the wireless channel (S_{21}), amplitude and phase, using an HP-8722ES network analyzer. We see the insertion loss of the channel increases with frequency. Operation at lower frequencies improves the BER performance of the system. Pulse shaping can help us to put more power of the transmitted pulse in lower frequency and increase link efficacy. Fig. 4 shows a photo of the measurement setup.

Isolation of the uplink transmitter from the downlink receiver in our implant is challenging. For the external unit we can use a discrete power divider with excellent isolation (22 dB in Fig. 3a). The implant requires an integrated solution. The UWB uplink transmitter in an integrated solution (on-chip) will naturally have very high impedance, providing isolation to the 2.45 GHz downlink receiver. In our experiment with discrete components (not integrated) we emulate this high isolation via a UWB bandpass filter (see Fig. 3a). The bandpass filter rejects the 2.45 GHz downlink signal, effectively routing all energy to the 2.45 GHz receiver.

To isolate the 2.45 GHz downlink receiver from transmitted UWB signal, we use pulse shaping for UWB pulse to have the lowest crosstalk with 2.45 GHz ISM band. Fig. 5a shows the measured UWB pulse with OOK modulation at the output of the AWG, as captured by the real-time oscilloscope. In Fig. 5b we see the spectrum for the UWB signal. The pulse is shaped to place energy between 3.1-7 GHz, and to introduce a notch at 2.45 GHz, yielding good isolation between uplink and downlink.

The final determination of the effectiveness of isolation is the bit error rate performance of uplink and downlink. We will see in the following sections that measured BER is close to theoretical limits, hence crosstalk is negligible.

IV. Modulation Options

To provide the systems designer maximum flexibility this architecture has the added advantage of supporting three signaling methods: OOK, BPSK and DPSK. Each modulation format is briefly described, including the required receiver.

A. BPSK Modulation

Phase-Shift Keying (PSK) is a modulation scheme in which the phase of a signal is varied to transmit information. In binary phase shift keying (BPSK) the phase of the signal is varied by 180 degrees with the polarity of the binary data. BPSK is detected by using a matched filter or the equivalent correlation receiver. To detect the received signal coherently a template pulse is needed for the correlation receiver as shown in Fig. 6. To generate the optimal template, the frequency response of the channel must be known [34]; the measured frequency response of the channel is plotted in Fig. 3-b. The transmitted, received and detected signals are shown in Fig. 7-a for 500 Mb/s and SNR=20 dB.

B. DPSK Modulation

DPSK modulation transmits data on changes in phase from symbol to symbol. Because the data are detected by correlation with a delayed version of the received waveform, the data must first be encoded in a differential fashion [34]. Self-homodyne detection (i.e., correlation with a delayed version of the received signal), is followed by integration and detection blocks as shown in Fig. 6-b. The transmitted, received and detected signals are shown in Fig. 7-b for 500 Mb/s and SNR=20 dB.

C. OOK Modulation

On-Off Keying (OOK) is the simplest form of amplitude-shift keying modulation. The presence of a waveform for a specific duration represents a binary one, while its absence for the same duration represents a binary zero [34]. For detection, the received signal is multiplied by itself, integrated and detected as shown in Fig. 6-c. The transmitted, received and detected signal for uplink are shown in Fig. 7-a for 500 Mb/s and SNR=20 dB. Also, the data transmission for downlink is presented in Fig. 7-d for 100 Mb/s and SNR=20 dB.

Fig. 6 shows the block diagram of the receiver systems for different modulations, performed offline in MATLAB on data captured by the real-time oscilloscope. For the uplink, Fig. 7 shows the modulated waveforms with random digital data at the transmitter, the receiver, and following detector. In Fig. 7 "Transmitted signal" is the waveform modulated with a PRBS of order 15 and 1 million bits length for different modulations which is uploaded in AWG. "Received signal" is the signal which is captured by real-time oscilloscope. "Filtered signal" is the captured signal after band-pass filter in Fig. 6. "Integrated

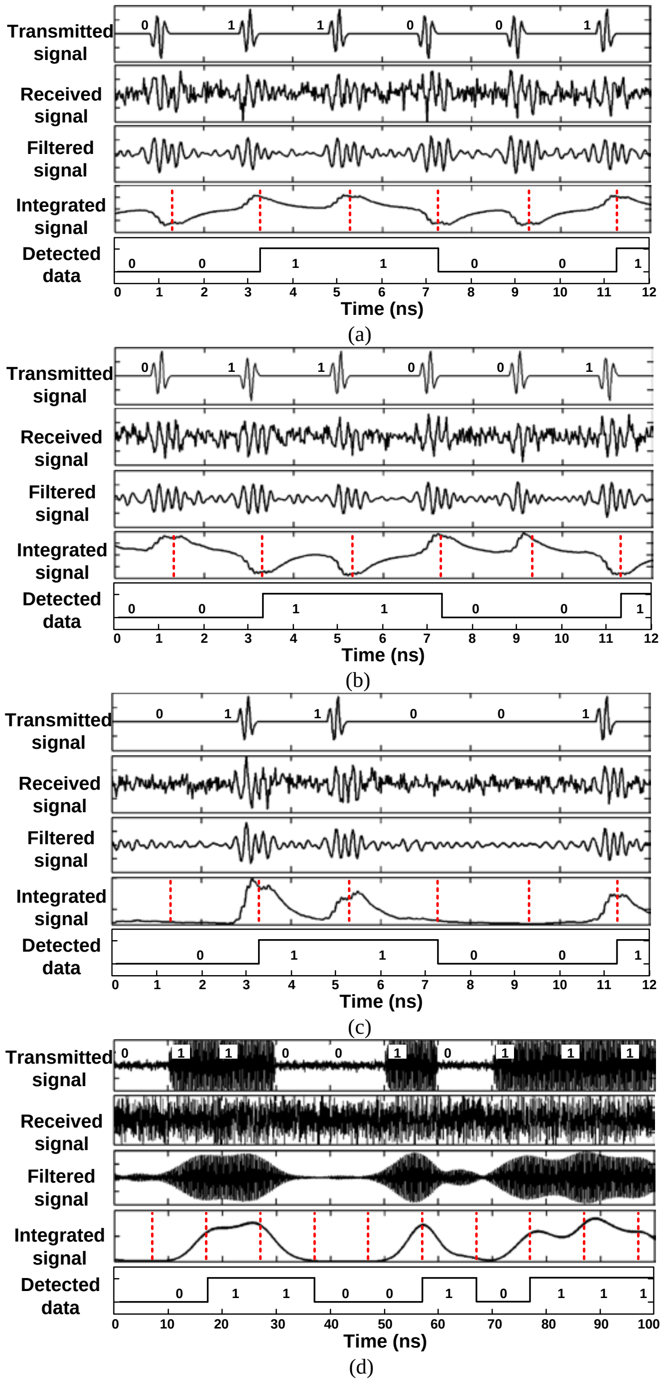

Fig. 7. Different stages of data transmission for (a) BPSK uplink, (b) DPSK uplink, (c) OOK uplink, and (d) OOK downlink.

signal" is the output of the integrator (a RC low-pass filter) in Fig. 6. The red dash-lines in the "Integrated signal" are the sampling times. In order to detect transmitted data, the sampled signal (dashed red line) is compared with a threshold value. "Transmitted signal" in Fig. 7-d refer to the downlink at output signal of the mixer which is captured by the real-time oscilloscope. "Received signal", "Filtered signal" and "Integral Signal" are similar to those discussed for the uplink. Discussions about different modulations are provided below.

V. Data Rates and BER performance

Recent neural research targets a large number of channels for neural recording and stimulating to enable better understanding of complex dynamic behavior [9, 37]. The reported data rates for neural recording in the UWB band are shown in Table I. Circuit design has been the primary focus of BMI research, with less attention on data transmission performance of implant-to-air communications. Recently data transmission of 80 Mbps in the UWB band was investigated for wireless implant-to-air data communications for gastro applications [21]. We were able to push data rates above the 80 Mbps by using more bandwidth in UWB band and because of less insertion loss for the BMI than the gastro application [38]. Our architecture improves the data rate, without penalty in power consumption, and retaining small-form factor and CMOS compatible solution. Here we describe the bit error rate performance at various data rates, both experimentally and in simulation.

Using the setup described in the previous section, transmitted data are captured by the real-time oscilloscope for UWB and 2.45 GHz links simultaneously. The BER is calculated and the BER vs. SNR of each link is presented in Fig. 8. Uplink BER appears in Fig. 8 a-c for BPSK, OOK and DPSK modulations at 500 Mb/s, 1 Gbps and 2 Gbps, respectively. The downlink BER is presented in Fig. 8-d for OOK modulation at 100 Mb/s.

The SNR penalties between modulation formats at 0.001 BER are shown in the Fig. 8. As expected, the best BER performance is obtained by BPSK. When the data rate is increased, the BER performance is reduced due to the ISI effect. Increasing the data rate leads to greater ISI and worse BER performance. However, equalization techniques can be used to solve this issue at rates above 500 Mb/s. As this processing would

TABLE I
Reported Brain Machine Interface Data Rate

Ref., Type of Link	BW (GHz)	Data rate (Gbps)	Modulation
[7], TX	3.1-5	90	OOK
[36], TX	3.1-5	200	PPM
[This work], TX	3.1-7	2000	OOK, BPSK DPSK
	Link type	Data rate (Mb/s)	Modulation
[This work], RX	RF	100	OOK
[37], RX	Inductive	1	ASK
[38], RX	Inductive	2.5	FSK
[39], RX	Inductive	2	DPSK

TABLE II
Average transmitted power at .001 BER for different receiver sensitivities for 500 Mb/s uplink and 100 Mb/s downlink

Receiver Sensitivity		-67 dBm	-40 dBm	-30 dBm	-15 dBm
UW-link TX-Power (dBm)	OOK	-17.3	9.7	19.7	34.7
	BPSK	-25.6	1.4	11.4	26.4
	DPSK	-21.46	5.54	15.54	30.54
Receiver Sensitivity		-47 dBm	-40 dBm	-30 dBm	-15 dBm
2.45 GHz-link TX-Power (dBm)	OOK	- 25.7	-18.7	-8.7	6.3

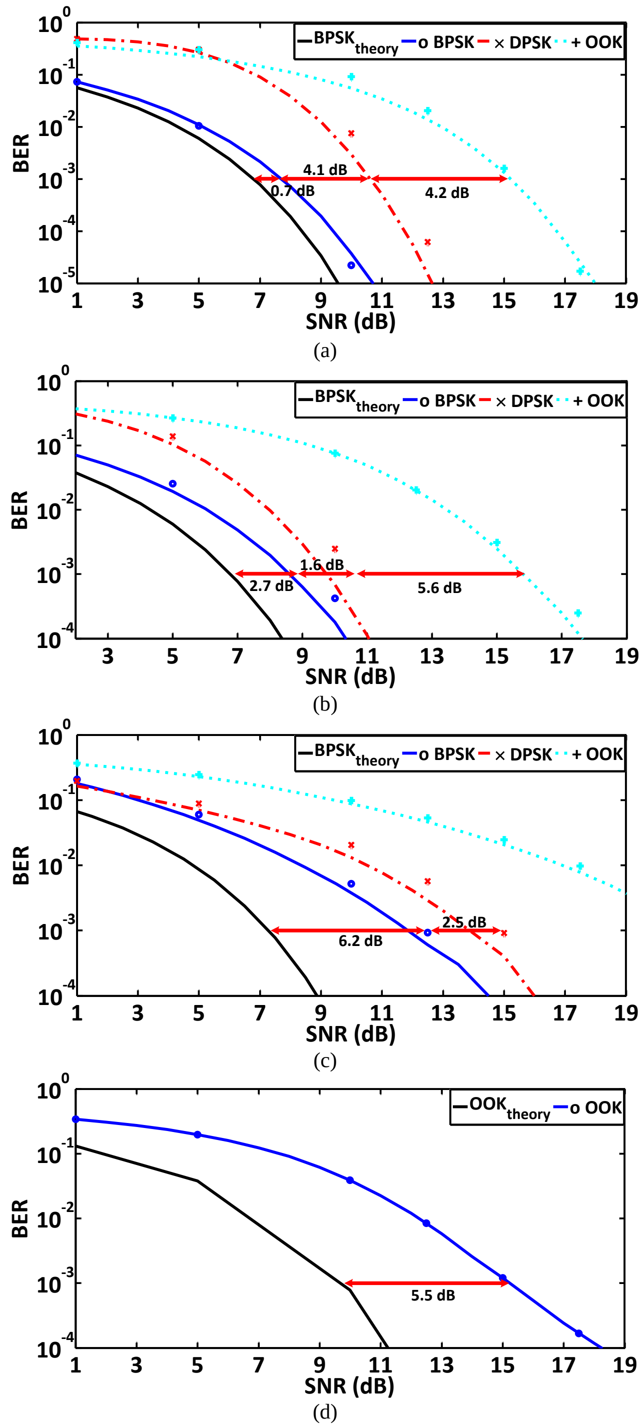

Fig. 8. BER for (a) 500 Mb/s uplink, (b) 1Gb/s uplink, (c) 2 Gb/s uplink, and (d) 100 Mb/s downlink link. Markers are measured BER, while continuous curves are simulations. Red arrows are SNR penalties at 10^{-3}; points at 10^{-3} in (a) are described in Table II.

occur in the external receiver, the added complexity is not burdensome. For the downlink, data rates are moderate, below 100 Mb/s, and equalization should not be necessary in the implant. The maximum data rate and the BER performance are plotted for this link in Fig. 8-d.

We use off-line process to emulate the external hardware for uplink detection, and the implanted receiver for the downlink. The receiver sensitivity in our off-line calculations are determined by the real time oscilloscope which it is high. We estimate the required transmit power to attain 0.001 BER with less ideal sensitivities, i.e., which can be implemented by CMOS circuits. The average of the transmitted power is calculated for different receiver sensitivities and is presented in Table I. These values are calculated at 500 Mb/s for the uplink and 100 Mb/s for the downlink.

In section II-D we found the maximum safe transmit power was 8 dBm for the uplink and 9.5 dBm for the downlink. Therefore for the 100 Mb/s downlink we can achieve .001 BER with any of the receiver sensitivities examined in Table II. For the 500 Mb/s uplink we are more limited. For BPSK and DPSK a receiver sensitivity of -40 dBm is required. For OOK greater sensitivity would be required. While Table II gives required power for 100 Mb/s uplink and 500 Mb/s uplink to achieve .001 BER at given receiver sensitivities, for other data rates and points on the BER curves of Fig. 8, the transmitted power can be calculated (as a function of the SNR and the data rate) to determine if ASAR limits are respected.

To reach our BER target for OOK with -40 dBm receiver sensitivity, we can place more power in lower frequency than 7 GHz and try to limit the spectrum of the optimized pulse (to a subband of 3.1-7 GHz) to increase the power efficiency and improve BER. Another solution is to reduce the data rate below 500 Mb/s. In other words, to keep average power constant while the energy per bit is increased, the data rate must be reduced.

Simulations were run to predict BER based on measured characteristics of the discrete components. The uplink pulse shapes, T_{x_uplink}, were generated in MATLAB, and were identical to those generated experimentally and uploaded to the arbitrary waveform generator. We used the frequency response, h(t), in Fig. 3b to simulate the overall channel (transceiver hardware, antennas and biological tissues). The receiver used detection algorithms identical to those used on captured experimental data (Fig. 6). We simulated simultaneous transmission of one million bits in both links (UWB and 2.45 GHz). The received pulses $R_{x\_downlink}$ and R_{x_uplink} for the uplink and downlink, respectively, were calculated from

$$(R_{x\_downlink}+R_{x\_uplink})=h(t)*(T_{x\_downlink}+T_{x\_uplink}) \qquad (1)$$

where $T_{x\_downlink}$ is the square wave OOK downlink signal. The simulated BER performance is in good agreement with measurements in Fig. 8 (experiment in markers, simulations in continuous curves). This agreement shows the frequency domain characterization is sufficient for predicting BER performance.

VI. Discussion of Integrated Circuit Solution

The experimental demonstration with discrete components confirms that the proposed architecture can indeed support the highest reported bit rates for BMI wireless transceivers. The utility of this architecture must also be validated in integrated solution. In this section we provide some additional information on the integrated solution with all components that has been sent for fabrication and will be used in later experiments.

The proposed full-duplex transceiver includes a 2.45 GHz OOK receiver and a UWB 3.1-7 GHz transmitter. Since both

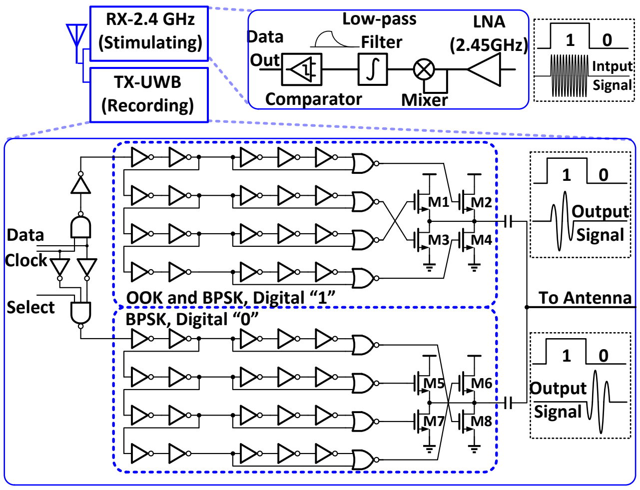

Fig. 9. Block diagram of an implantable full-duplex transceiver including UWB transmitter and 2.45 GHz receiver.

the receiver and the transmitter use the same antenna and communicate simultaneously on different frequency bands for this application, our solution decreases design complexity and the total size of the implanted device. The block diagram of the 2.45 GHz OOK receiver component (reported in [18]) is shown in Fig. 9. The input signal is amplified by the LNA, down-converted to baseband and low-pass filtered before being digitized by a comparator.

A customized circuit shown in Fig. 9 sculpts the UWB pulses by adjusting the amplitude and the time duration of the 5^{th} derivatives of a Gaussian pulse. Several time-shifted glitch pulses are summed to form the UWB pulses [5, 33]. The UWB transmitter circuit uses regular CMOS logic gates, such as inverters and NORs, and NMOS transistors. Four inverter-based delay lines shift the generated pulses. The four shifted impulses are output via transistors M1-M4, to form the required UWB signal data transmission.

OOK modulation is produced when only the top half of the circuit is active. For BPSK modulation, the same circuit with a different output configuration produces impulses with a 180° phase difference using the bottom half of the circuits depicted in Fig. 3. Digital "1" are produced by the top circuit, while digital "0", which corresponds to the 180°-phase shifted impulses, are produced by the bottom circuit. DPSK modulation has same transmitter as BPSK but it needs a precoding before transmitting [34].

VII. Conclusion

Designing a reliable wireless high speed data link in the presence of lossy biological tissues is a challenging task. We proposed a new wireless communications architecture for implanted systems that simultaneously stimulate neurons and record neural responses. The proposed full-duplex dual-band transceiver configuration avoids using a circulator or a conventional diplexer and includes only one data link which makes the implanted integrated transceiver more compact and power efficient at the circuit level. This architecture can support a large number of electrodes (>500), providing 100 Mb/s for the downlink of stimulation signals, and Gb/s for the uplink neural recordings.

We presented an ex-vivo experiment using discrete components achieving Gb/s uplink rates. The BER performance of BPSK, OOK and DPSK were investigated with the 5th derivative of a Gaussian pulse as the uplink UWB waveform. The BER performance of OOK was examined for the downlink. A receiver sensitivity of -40 dBm is required for BPSK and DPSK to achieve BER of 10^{-3} at 500 Mb/s for the uplink. For the OOK downlink at 100 Mb/s a receiver sensitivity of -15 dBm is sufficient. Future work will focus first implementing the circuit level of this new architecture. Our group is working on designing and optimizing the other blocks [43, 44] of brain machine interface system. The ultimate goal is to have an integrated solution to test the neural recording and stimulation system in-vivo.

References

[1] B. Gosselin, "Recent Advances in Neural Recording Microsystems," *Sensors*, vol.11, pp. 4572-4597, 2011.

[2] B. Gosselin, A.E. Ayoub, J.F. Roy, M. Sawan, F. Lepore, A. Chaudhuri, and D. Guitton, "A Mixed-Signal Multichip Neural Recording Interface With Bandwidth Reduction," *IEEE Transactions on Biomedical Circuits and Systems*, vol.3, pp.129-141, 2009.

[3] N.M. Neihart and R.R. Harrison, "Micropower circuits for bidirectional wireless telemetry in neural recording applications, " *IEEE Transactions on Biomedical Engineering*, vol.52, pp.1950-1959, 2005.

[4] Y. Gao, Y. Zheng, S. Diao, W.D. Toh, C.W. Ang, M. Je, and C.H. Heng," Low-power ultrawideband wireless telemetry transceiver for medical sensor applications,"*IEEE Transactions on Biomedical Engineering*, vol.58, no.3, pp.768-772, 2010.

[5] H. Miranda and T.H. Meng, "A programmable pulse UWB transmitter with 34% energy efficiency for multichannel neuro-recording systems," *IEEE Custom Integrated Circuits Conference (CICC)*, vol.1, no.4, pp.19-22, 2010.

[6] H. Zamani and P. Mohseni," A high-speed circuit architecture for IR-UWB transmission of fast-scan cyclic voltammetry in 0.35 um CMOS," *IEEE Engineering in Medicine and Biology Society (EMBC'10)*, pp.1561-1564, 2010.

[7] M.S. Chae, Z. Yang, M.R. Yuce, L. Hoang, and W. Liu, "A 128-Channel 6 mW Wireless Neural Recording IC With Spike Feature Extraction and UWB Transmitter," *IEEE Transactions on Neural Systems and Rehabilitation Engineering*, vol.17, no.4, 2009.

[8] U.M. Jow and M. Ghovanloo,"Optimization of Data Coils in a Multiband Wireless Link for Neuroprosthetic Implantable Devices," *IEEE Transaction on Biomedcal Circuits and System*, vol.4, no.5, 2010.

[9] Y. Kuan, Y. Lo, Y. Kim, M.F. Chang, and W. Liu, "Wireless Gigabit Data Telemetry for Large-Scale Neural Recording," *IEEE Journal of Biomedical and Health Informatics*, vol.19, no.3, pp.949-957, 2015.

[10] H. Schwerdt, W. Xu, S. Shekhar, A. Abbaspour-Tamijani , B.C. Towe, F.A. Miranda, and J. Chae, " A Fully Passive Wireless Microsystem for Recording of Neuropotentials Using RF Backscattering Methods," *IEEE/ASME Journal of Microelectromechanical Systems*, vol.20, no.5, pp.1119-1130, 2011.

[11] H. Schwerdt, F.A. Miranda, and J. Chae, " A Fully Passive Wireless Backscattering Neuro-Recording Microsystem Embedded in Dispersive Human Head Phantom Medium," *IEEE Electron Devices Letters*, vol.33, no.6, pp.908-910, 2012.

[12] H. Schwerdt, F.A. Miranda, and J. Chae, "Analysis of Electromagnetic Fields Induced in Operation of a Wireless Fully Passive Backscattering Neurorecording Microsystem in Emulated Human Head Tissue," *IEEE Transactions on Microwave Theory and Techniques*, vol.61, no.5, pp.2170-2176, 2013.

[13] D.A. Borton , M. Yin , J. Aceros, and A. Nurmikko, "An implantable wireless neural interfacefor recording cortical circuit dynamics in moving primates," *Journal of Neural Engineering*, vol.10, no.2, pp.026010, 2013.

[14] C.W.L. Lee, A. Kiourti, J. Chae, and J.L.Volakis, "A High-Sensitivity Fully Passive Neurosensing System for Wireless Brain Signal Monitoring," *IEEE Transactions on Microwave Theory and Techniques*, vol.63, no.6, pp.2060-2068, 2015.

[15] S. Rao, N. Llombart, E. Moradi, K. Koski, T. Bjorninen, L. Sydanheimo, J.M. Rabaey, J.M. Carmena, Y. Rahmat-Samii, and L. Ukkonen, "Miniature implantable and wearable on-body antennas: towards the new era of wireless body-centric systems," *IEEE Antennas and Propagation Magazine*, vol.56, no.1, pp.271-291, 2014.

[16] G. Simard, M. Sawan, and D. Massicotte, "Novel coils topology intended for biomedical implants with multiple carrier inductive link," *IEEE International Symposium on Circuits and Systems (ISCAS),* pp.537-540, 2009.

[17] G. Simard, M. Sawan, and D. Massicotte,"High-Speed OQPSK and Efficient Power Transfer Through Inductive Link for Biomedical Implants," *IEEE Transactions on Biomedical Circuits and Systems*, vol.4, no.3, pp.192-200, 2010.

[18] S.A. Mirbozorgi, H. Bahrami, L.A. Rusch, and B. Gosselin, "A Low-Power 2.4-GHz Receiver for Wireless Implantable Neural Stimulators," *IEEE International Symposium on Circuits and Systems (ISCAS)*, pp.1082-1085, 2014.

[19] H. Bahrami, S.A. Mirbozorgi, R. Ameli, L.A. Rusch, and B. Gosselin, "Flexible, Polarization-Diverse UWB Antennas for Implantable Neural Recording Systems," *IEEE Transactions on Biomedical Circuits and Systems*, vol.PP, no.99, pp.1,1, 2015.

[20] H. Bahrami, S.A. Mirbozorgi, L.A. Rusch, B. Gosselin, "Biological Channel Modeling and Implantable UWB Antenna Design for Neural Recording Systems," *IEEE Transactions on Biomedical Engineering*, vol.62, no.1, pp.8-98, 2015.

[21] R. Chavez-Santiago, et al.,"Experimental implant communication of high data rate video using an ultra wideband radio link," *35th Annual International Conference of the IEEE Engineering in Medicine and Biology Society (EMBC)*, 2013.

[22] S.C. Shin, J.Y. Huang, K.Y. Lin, and H. Wang,"A 1.5–9.6 GHz Monolithic Active Quasi-Circulator in 0.18 µm CMOS Technology," *IEEE Microwave and Wireless Components Letters*, vol.18, no.12, pp.797-799, 2008.

[23] Z. E. Khatib, L. MacEachern, and S.A. Mahmoud,"A fully-integrated linearized CMOS bidirectional distributed amplifier as UWB active circulator," *International Conference on Microelectronics (ICM)*, pp.106-109, 2008.

[24] S. He, N. Akel, and C.E.Saavedra,"Active quasi-circulator with high port-to-port isolation and small area," *Electronics Letters*, vol.48, no.14, pp.848-850, 2012.

[25] H. Morkner, M. Karakucuk, G. Carr, and S. Espino,"A full duplex Front End Module for WiFi 802.11.n applications," *European Conference on Wireless Technology (EuWiT)*, pp.162-165, 2008.

[26] Y. Tae-Yeoul, W. Chunlei, P. Zepeda, C.T. Rodenbeck, M.R. Coutant, L. Ming-Yi, and C. Kai,"A 10- to 21-GHz, low-cost, multi-frequency, and full-duplex phased-array antenna system," *IEEE Transactions on Antennas and Propagation*, vol.50, no.5, pp. 641-650, 2002.

[27] O. Kyujin, S. Sankaran, W. Hsin-Ta, L. Jau-Jr, H. Minsoon, and K.O. Kenneth,"Full-Duplex Crystalless CMOS Transceiver With an On-Chip Antenna for Wireless Communication in a Hybrid Engine Controller Board," *IEEE Journal of Solid-State Circuits*, vol.48, no.6, pp.1327-1342, 2013.

[28] X. Zhang, M. Elgamel, and M.A. Bayoumi,"Gaussian pulse approximation using standard CMOS and its application for sub-GHz UWB impulse radio," *International Journal of Circuit Theory and Applications*, vol.38, no.4, 2008.

[29] D. D. Wentzloff,"Pulse-based ultra-wideband transmitters for digital communication," Ph.D. dissertation, Massachusetts Inst. Technol. (MIT), 2007, *(http://dspace.mit.edu/handle/1721.1/40546).*

[30] Demirkan, M.; Spencer, R.R.,"A Pulse-Based Ultra-Wideband Transmitter in 90-nm CMOS for WPANs," *IEEE Journal of Solid-State Circuits*, vol.43, no.12, pp.2820-2828, 2008.

[31] Y. Zhu, J.D. Zuegel, J.R. Marciante, and H. Wu," Distributed Waveform Generator: A New Circuit Technique for Ultra-Wideband Pulse Generation, Shaping and Modulation," *IEEE Journal of Solid-State Circuits*, vol.44, no.3, 2009.

[32] L. Zhou, Z. Chen, C.C. Wang, F. Tzeng, V. Jain, and P. Heydari, " A 2-Gb/s 130-nm CMOS RF-Correlation-Based IR-UWB Transceiver Front-End," *IEEE Transactions on Microwave Theory and Techniques*, vol.59, no.4, 2011.

[33] K. Hyunseok and J. Youngjoong, "Fifth-derivative Gaussian pulse generator for UWB system," *IEEE Radio Frequency integrated Circuits (RFIC) Symposium*, pp.671-674, 2005.

[34] B. Sklar, *Digital Communications: Fundamentals and Applications*, Prentice Hall, , 2nd edition, 2001.

[35] "IEEE Standard for Safety Levels with Respect to Human Exposure to Radio Frequency Electromagnetic Fields, 3 kHz to 300 GHz," *IEEE Standard*, C95.1-2005, 2006.

[36] A. Drossos, V. Santomaa, and N. Kuster,"The Dependence of Electromagnetic Energy Absorption Upon Human Head Tissue Composition in the Frequency Range of 300–3000 MHz," *IEEE Transaction on Microwave Theory and Techniques*, vol.48, no.11, 2000.

[37] D.A. Schwarz, M.A. Lebedev, T.L. Hanson, D.F. Dimitrov, G. Lehew, J. Meloy, S. Rajangam,V. Subramanian, P.J. Ifft, Z. Li, A. Ramakrishnan, A. Tate, K.Z. Zhuang, and M. A.L. Nicolelis,"Chronic, wireless recordings of large-scale brain activity in freely moving rhesus monkeys," *Nature Methods*, vol.11, pp. 670–676, 2014.

[38] H. Bahrami, S.A. Mirbozorgi, L.A. Rusch, and B. Gosselin, "BER Performance of Implant-to-Air High-Speed UWB Data Communications for Neural Recording Systems," *36th Annual International Conference of the IEEE Engineering in Medicine and Biology Society (EMBC)*, 2014.

[39] O. Novak, W. Wu, and C. Charles,"Wireless ultra-wide-band data link for biomedical implants," *Research in Microelectronics and Electronics (PRIME)*, pp. 352-355, 2009.

[40] G. Yilmaz, O. Atasoy, C. Dehollain,"Wireless Energy and Data Transfer for In-Vivo Epileptic Focus Localization," *IEEE Sensors Journal*, vol.13, no.11, pp.4172-4179, 2013.

[41] M. Ghovanloo and K. Najafi,"A Wireless Implantable Multichannel Microstimulating System-on-a-Chip With Modular Architecture," *IEEE Transactions on Neural Systems and Rehabilitation Engineering*, vol.15, no.3, pp.449,457, 2007.

[42] K. Chen, Z. Yang, L. Hoang, J. Weiland, M. Humayun, and W. Liu,"An Integrated 256-Channel Epiretinal Prosthesis," *IEEE Journal of Solid-State Circuits*, vol.45, no.9, pp.1946–1956, 2010.

[43] X. Liu, M. Zhang, B. Subei, A.G. Richardson, T.H. Lucas, and J.V.d. Spiegel, "The PennBMBI: Design of a General Purpose Wireless Brain-Machine-Brain Interface System," *IEEE Transactions on Biomedical Circuits and Systems*, vol.9, no.2, pp.248-258, 2015.

[44] F. Shahrokhi, K. Abdelhalim, D. Serletis, P.L. Carlen, and R. Genov, "The 128-Channel Fully Differential Digital Integrated Neural Recording and Stimulation Interface," *IEEE Transactions on Biomedical Circuits and Systems*, vol.4, no.3, pp.149-161, 2010.

Hadi Bahrami (S'12) received the B.S. and M.S. degrees in electrical engineering 2005 and 2007 from Isfahan University of Technology, Isfahan, Iran and Tarbiat Modares University, Tehran, Iran, respectively. He was a PhD student in 2011-2015 at Université Laval, Québec, Canada. He is currently pursuing a Postdoc at the Center for Optics, Photonics and Lasers (COPL), Université Laval, Canada. His interests are radio frequency integrated circuit (RFIC) and photonic integrated circuit (PIC) for wireless and optical communications.

S. Abdollah Mirbozorgi (S'10) received the B.S. degree from the Noshirvani University of Technology, Babol, Iran, and the M.S. degree from the Ferdowsi University of Mashhad, Mashhad, Iran, both in electrical engineering, in 2008 and 2011, respectively. Currently, he is working toward the Ph.D. degree in the Biomedical Microsystems Laboratory, Department of Electrical and Computer Engineering, Universite Laval, Québec, QC, Canada. His interests include neural and bionic implants, wireless implantable biomedical systems, integrated analog circuit design, and wireless power/data transmission.

An T. Nguyen was born in 1982. He received the B.S. degree in physics in 2003 and M.S. degree in electronics engineering in 2007 from University of Science – Vietnam National University (VNU) in Ho Chi Minh City, Vietnam. From 2008 to 2011, he was pursuing his Ph.D. degree in optical telecommunications at the Centro di Eccellenza per l'Ingegneria dell'Informazione, della Comunicazione e della Percezione (CEIICP) of Scuola Superioré Sant'Anna, Pisa, Italy. His research topics involved ultra-fast (640Gbps and beyond) OTDM subsystems, multifunctional hybrid add/drop node for OTDM and WDM integration, all-optical wavelength and modulation format converter, ultrafast packet switching and photonic digital processing circuits. From 2012 to 2015, he was a post-doc at the Centre d'Optique, Photonique et Laser (COPL), Université Laval, Québec, Canada. His projects focus on optical coherent detection systems with higher-order modulation formats, OFDM-over-fiber and full-duplex wireless-fiber interfacing. He is currently with Infinera Corp., California, United States, as a test developing engineer for new generations of photonic integrated circuit employed in coherent long-haul and metro communication systems.

Benoit Gosselin (S'02–M'08) obtained the M.Sc. and Ph.D. degrees both in Electrical Eng. from École Polytechnique de Montréal, Montréal, QC, Canada, in 2009. He held a mixed-signal layout design position at PMC Sierra Inc., Montreal in 2009, and he was an NSERC Postdoctoral Fellow at the Georgia Institute of Technology in 2010. Dr. Gosselin is currently Associate Professor at the Department of ECE at Laval University, Quebec City, QC, Canada, where he is heading the Biomedical Microsystems Lab. His research has generated more than 70 articles published in journals and international conferences, 5 book chapters and 3 patent applications, which have been cited over 600 times per Google Scholar. He organized and chair sessions in several international conferences, and he served on the Technical Committees of IEEE BIOCAS, IEEE NEWCAS, IEEE EMBC, and IEEE ISCAS. Dr Gosselin regularly serves as a referee for renowned journals and major conferences in the area of circuits and systems and biomedical engineering. He is Founder and Chair of the CAS/EMB Chapter and Vice-Chair of the Computer Chapter of the IEEE Quebec Section. He is a member of the Executive committee and Representative Member on the Board of Directors for Université Laval of the Microsystems Strategic Alliance of Québec (ReSMiQ), which regroups 40 researchers and more than 200 students involved in microsystems research. His research interests include VLSI circuits for bioinstrumentation, wireless biosensing, implantable electronics, brain computer interfaces and low-power analog/mixed-mode integrated circuits design.

Leslie A. Rusch (S'91–M'94–SM'00–F'10) received the B.S.E.E. degree (with honors) from the California Institute of Technology, Pasadena, in 1980 and the M.A. and Ph.D. degrees in electrical engineering from Princeton University, Princeton, NJ, in 1992 and 1994, respectively. She currently holds a Canada Research Chair in Communications Systems Enabling the Cloud in the Department of Electrical and Computer Engineering at Université Laval, QC, Canada. She is an IEEE Fellow and a member of the Centre for Optics, Photonics and Lasers at UL. Dr. Rusch has experience in defense, industrial and academic communications research. She was a communications project engineer for the Department of Defense from 1980-1990. While on leave from Université Laval, she spent two years (2001-2002) at Intel Corporation creating and managing a group researching new wireless technologies. Prof. Rusch's research interests include digital signal processing for coherent detection in optical communications, spatial multiplexing using orbital angular momentum modes in fiber, radio over fiber and OFDM for passive optical networks; and in wireless communications, optimization of the optical/wireless interface in emerging cloud based computing networks, and implantable medical sensors with high bit rate UWB telemetry. She is recipient of the IEEE Canada J. M. Ham Award for Graduate Supervision. Prof. Rusch has published over 120 journal articles in international journals (90% IEEE/OSA) with wide readership, and contributed to over 150 conferences. Her articles have been cited over 4000 times per Google Scholar.